

An Interaction Integral Method for Computing Fracture Parameters in Functionally Graded Magnetoelastic Composites

J. Sladek¹, V. Sladek¹, P. Stanak¹, Ch. Zhang² and M. Wünsche²

Abstract: A contour integral method is developed for the computation of stress intensity, electric and magnetic intensity factors for cracks in continuously non-homogeneous magnetoelastic solids under a transient dynamic load. It is shown that the asymptotic fields in the crack-tip vicinity in a continuously nonhomogeneous medium are the same as in a homogeneous one. A meshless method based on the local Petrov-Galerkin approach is applied for the computation of the physical fields occurring in the contour integral expressions of intensity factors. A unit step function is used as the test functions in the local weak-form. This leads to local integral equations (LIEs) involving only contour-integrals on the surfaces of subdomains. The moving least-squares (MLS) method is adopted for approximating the physical quantities in the LIEs. The accuracy of the present method for computing the stress intensity factors (SIF), electrical displacement intensity factors (EDIF) and magnetic induction intensity factors (MIIF) are discussed by comparison with numerical solutions for homogeneous materials.

Keywords: Smart materials, Fracture, Computational modelling, Numerical analysis, Moving least-squares approximation

1 Introduction

Functional composite materials, such as piezoelectric, magnetostrictive and thermoelastic composites are being rapidly developed with increasing applications in ultrasonic imaging devices, sensors, actuators and transducers etc. Such composites inherit the characteristics of functional materials, such as the piezoelectric and piezomagnetic properties which can be tailored to meet specific applications. Modern smart structures made of piezoelectric and piezomagnetic mate-

¹ Institute of Construction and Architecture, Slovak Academy of Sciences, 84503 Bratislava, Slovakia

² Department of Civil Engineering, University of Siegen, D-57068 Siegen, Germany

rials offer certain potential performance advantages over conventional ones due to their capability of converting the energy from one type to other (among magnetic, electric, and mechanical) (Avellaneda and G. Harshe, 1994; Landau et al., 1984; Nan, 1994). However, one great drawback of piezoelectric and piezomagnetic materials is their inherent brittleness (ultimate strength $< 100 \text{ MPa}$) and low fracture toughness ($0.5\text{--}2.0 \text{ MPa}\sqrt{m}$). Furthermore, highly inhomogeneous and concentrated stresses, electrical and magnetic fields may occur inside the smart structures and composites due to fabrication or operational loads. Therefore, much attention has been devoted to fracture mechanics of piezoelectric, ferroelectric and magneto-electroelastic materials for the last 20 years. Following papers (Gao et al. 2003; Hu et al. 2006; Song and Sih 2003; Tian and Gabbert 2005; Tian and Rajapakse 2005; Wang et al. 2006; Wang and Mai 2007; Zhou et al. 2004) are interesting in fracture of 2D problems under a static load. Dynamic fracture analyses of magneto-electroelastic solids are sparse and they are mostly restricted to a relatively simple anti-plane problem (Du et al. 2004; Feng and Su 2006,2007; Guo et al. 2009; Li and Lee 2008; Ma et al. 2007,2009; Su and Feng 2007).

New structural concepts have emerged where multifunctional materials, exhibiting a strong coupling between its mechanical response and its electrical, magnetic or thermal behaviour, which can work as sensors and actuators. These structures are termed as adaptive structures. It has been observed that remarkably large magneto-electric effects are observed for composites than for either composite constituent (Nan, 1994; Feng and Su, 2006). If the volume fraction of the constituents is varying in a predominant direction we are talking about functionally graded materials (FGMs). Originally these materials have been introduced to benefit from the ideal performance of its constituents, e.g. high heat and corrosion resistance of ceramics on one side, and large mechanical strength and toughness of metals on the other side. A review on various aspects of FGMs can be found in the monograph of Suresh and Mortensen (1998) and the review chapter by Paulino et al. (2003). The FGM multiferroic model would result in substantial variations in magnetic parameters (magnetization, anisotropy, permeability and magnetostriction) (Han et al. 2006; Ueda 2003; Zhu et al. 1995). Unfortunately, all published crack analyses in continuously nonhomogeneous magneto-electroelastic materials have been restricted to anti-plane mechanical deformation (Feng and Su 2006, 2007; Guo et al. 2009; Li and Lee 2008; Ma et al. 2007,2009).

Advanced numerical methods are required to solve general boundary value problems for continuously nonhomogeneous magneto-electroelastic solids. It is due to the high mathematical complexity following from coupling of fields and spatial variation of material properties. In recent years, meshless formulations are becoming popular due to their high adaptability and low costs to prepare input and

output data in numerical analysis. The moving least squares (MLS) approximation is generally considered as one of many schemes to interpolate discrete data with a reasonable accuracy. Meshless methods can easily simulate crack propagation without remeshing (Li and Liu 2004). A variety of meshless methods has been proposed so far with some of them being applied for modeling of smart materials (Liu et al. 2002; Ohs and Aluru 2001; Sladek et al. 2007a, 2007b, 2008). The meshless local Petrov-Galerkin (MLPG) method is a fundamental base for the derivation of many meshless formulations, since trial and test functions can be chosen from different functional spaces. Recently, the MLPG method with a Heaviside step function as the test functions (Atluri 2004; Atluri et al. 2003) has been applied to solve two-dimensional (2-D) homogeneous piezoelectric problems (Sladek et al. 2006).

The MLPG method is applied, in the present paper, to solve 2-D continuously non-homogeneous magneto-electroelastic solids with cracks. The weak-forms for the coupled governing partial differential equations on small subdomains with a Heaviside step function as the test functions are applied to derive local integral equations. Applying the Gauss divergence theorem to the weak-forms, the local boundary-domain integral equations are derived. The spatial variations of the displacements, electric and magnetic potentials are approximated by the MLS (Atluri 2004; Belytschko et al. 1996). After performing the spatial MLS approximation, a system of ordinary differential equations for certain nodal unknowns is obtained. Then, the system of the ordinary differential equations of the second order resulting from the equations of motion is solved by the Houbolt finite-difference scheme (Houbolt 1950) as a time-stepping method.

Intensity factors for cracks in piezoelectric and magneto-electroelastic solids are mostly evaluated from the asymptotic expansion of the physical fields in the crack-tip vicinity (Garcia-Sanchez et al. 2007; Sladek et al. 2008). However, from elastic analyses it is well known that the accuracy of the computed stress and displacement fields in the crack-tip vicinity is lower than far away from the crack-tip (Kim and Paulino 2003). Cherepanov (1979) presented invariant integrals from which it is possible to derive the J-integral for piezoelectric materials. Later Pak and Herrmann (1986) derived a path independent integral for nonlinear dielectric materials. For piezoelectric materials, the J-integral was derived on the base of the electric enthalpy density (Pak 1990). Kim and Paulino (2003, 2004) computed the stress intensity factors (SIFs) and T-stress in orthotropic FGMs using the FEM by the interaction integral method. Similar procedure has been applied to derive conservation integrals for the evaluation of intensity factors in piezoelectric materials by Enderlein et al. (2005), Rao and Kuna (2008a) and to magneto-electroelastic ones (Rao and Kuna 2008b). Independently, Banks-Sills et al. (2008) have derived

a conservation integral for the evaluation of the intensity factors associated with piezoelectric materials for impermeable crack-face conditions. Motola and Banks-Sills (2009) have extended the conservation integral for calculating intensity factors for cracked piezoelectric ceramics using the exact boundary conditions on the crack-faces. All presented conservation integral methods are based on the domain integral form. Therefore, those methods are more convenient as post-processors to numerically obtained fields by domain discretization techniques. In the present paper we present conservation integrals in contour-domain integral form for continuously nonhomogeneous magneto-electroelastic solids. Only the inertial term and gradients of the material parameters contribute to the domain integrals. These terms are vanishing for a steady-state and homogeneous material case. Thus, the conservation integral expression is dominantly given by the contour integral. The accuracy of the contour integral method is very high for the present meshless method, since its path can be chosen sufficiently far from the crack-tip.

The accuracy and the efficiency of the proposed MLPG method are verified by several numerical examples for computing the stress intensity factors (SIF), electrical displacement intensity factor (EDIF) and magnetic induction intensity factor (MIIF). Numerical results are presented and compared with BEM solutions for homogeneous materials.

2 Asymptotic fields in the crack-tip vicinity in FGMs

The basic equations of phenomenological theory of linear magneto-electroelastic materials consist of the governing equations (Maxwell equations and the balance of momentum) and the constitutive relations. The governing equations completed by the boundary and initial conditions should be solved for unknown primary field variables such as the elastic displacement field $u_i(\mathbf{x}, \tau)$, the electric potential $\psi(\mathbf{x}, \tau)$ (or its gradient called the electric vector field $E_i(\mathbf{x}, \tau)$), and the magnetic potential $\mu(\mathbf{x}, \tau)$ (or its gradient called the magnetic intensity field $H_i(\mathbf{x}, \tau)$). The constitutive equations co-relate the primary fields $\{u_i, E_i, H_i\}$ with the secondary fields $\{\sigma_{ij}, D_i, B_i\}$ which are the stress field, the electric displacement field, and the magnetic induction field, respectively. The governing equations give not only the relationships between the conjugated fields in each of the pairs $(\sigma_{ij}, \varepsilon_{ij}), (D_i, E_i), (B_i, H_i)$ but describe also the magneto-electroelastic interactions in the phenomenological theory of continuous solids.

Taking into account the typical material coefficients, it can be found that the characteristic frequencies for elastic and electromagnetic processes are $f_{el} = 10^4 \text{Hz}$ and $f_{elm} = 10^7 \text{Hz}$, respectively. Thus, if we consider such solids under transient loadings with temporal changes corresponding to f_{el} , the changes of the electromagnetic fields can be assumed to be immediate, or in other words the electromagnetic

fields can be considered like quasi-static [57]. Then, the Maxwell equations are reduced to two scalar equations

$$D_{j,j}(\mathbf{x}, \tau) - R(\mathbf{x}, \tau) = 0, \quad (1)$$

$$B_{j,j}(\mathbf{x}, \tau) = 0, \quad (2)$$

where R is the volume density of free charges, and τ denotes the time variable.

The remaining vector Maxwell equations in the quasi-static approximation, $\nabla \times \mathbf{E} = 0$ and $\nabla \times \mathbf{H} = 0$, are satisfied identically by an appropriate representation of the fields $\mathbf{E}(\mathbf{x}, \tau)$ and $\mathbf{H}(\mathbf{x}, \tau)$ as gradients of the scalar electric and magnetic potentials $\psi(\mathbf{x}, \tau)$ and $\mu(\mathbf{x}, \tau)$, respectively,

$$E_j(\mathbf{x}, \tau) = -\psi_{,j}(\mathbf{x}, \tau), \quad (3)$$

$$H_j(\mathbf{x}, \tau) = -\mu_{,j}(\mathbf{x}, \tau). \quad (4)$$

To complete the set of the governing equations, eqs. (1) and (2) need to be supplemented by the equation of motion in the elastic continuum

$$\sigma_{i,j,j}(\mathbf{x}, \tau) + X_i(\mathbf{x}, \tau) = \rho \ddot{u}_i(\mathbf{x}, \tau), \quad (5)$$

where \ddot{u}_i , ρ and X_i denote the acceleration of the displacements, the mass density, and the body force vector, respectively. A comma after a quantity represents the partial derivatives of the quantity and a dot is used for the time derivative.

The constitutive relations represent the coupling of the mechanical and the electromagnetic fields. They can be obtained as derivatives of the electromagnetic enthalpy density defined by

$$W(\varepsilon_{ij}, E_i, H_i, \mathbf{x}) = \frac{1}{2} c_{ijkl}(\mathbf{x}) \varepsilon_{ij}(\mathbf{x}) \varepsilon_{kl}(\mathbf{x}) - e_{ikl}(\mathbf{x}) E_i(\mathbf{x}) \varepsilon_{kl}(\mathbf{x}) - \frac{1}{2} h_{ij}(\mathbf{x}) E_i(\mathbf{x}) E_j(\mathbf{x}) - d_{jkl}(\mathbf{x}) H_j(\mathbf{x}) \varepsilon_{kl}(\mathbf{x}) - \alpha_{jk}(\mathbf{x}) E_j(\mathbf{x}) H_k(\mathbf{x}) - \frac{1}{2} \gamma_{jk}(\mathbf{x}) H_j(\mathbf{x}) H_k(\mathbf{x}). \quad (6)$$

The constitutive equations involving the general magneto-electroelastic interaction (Nan 1994) in media with spatially dependent material coefficients for continuously non-homogeneous media can be written as

$$\sigma_{ij}(\mathbf{x}, \tau) = \frac{\partial W}{\partial \varepsilon_{ij}} = c_{ijkl}(\mathbf{x}) \varepsilon_{kl}(\mathbf{x}, \tau) - e_{kij}(\mathbf{x}) E_k(\mathbf{x}, \tau) - d_{kij}(\mathbf{x}) H_k(\mathbf{x}, \tau), \quad (7)$$

$$D_j(\mathbf{x}, \tau) = -\frac{\partial W}{\partial E_j} = e_{jkl}(\mathbf{x}) \varepsilon_{kl}(\mathbf{x}, \tau) + h_{jk}(\mathbf{x}) E_k(\mathbf{x}, \tau) + \alpha_{jk}(\mathbf{x}) H_k(\mathbf{x}, \tau), \quad (8)$$

$$B_j(\mathbf{x}, \tau) = -\frac{\partial W}{\partial H_j} = d_{jkl}(\mathbf{x})\varepsilon_{kl}(\mathbf{x}, \tau) + \alpha_{kj}(\mathbf{x})E_k(\mathbf{x}, \tau) + \gamma_{jk}(\mathbf{x})H_k(\mathbf{x}, \tau), \quad (9)$$

with the strain tensor ε_{ij} being related to the displacements u_i by

$$\varepsilon_{ij} = \frac{1}{2}(u_{i,j} + u_{j,i}). \quad (10)$$

The functional coefficients $c_{ijkl}(\mathbf{x})$, $h_{jk}(\mathbf{x})$ and $\gamma_{jk}(\mathbf{x})$ are the elastic coefficients, dielectric permittivities, and magnetic permeabilities, respectively; $e_{kij}(\mathbf{x})$, $d_{kij}(\mathbf{x})$ and $\alpha_{jk}(\mathbf{x})$ are the piezoelectric, piezomagnetic, and magnetoelectric coefficients, respectively. Owing to transient loadings, inertial effects and coupling, the elastic fields as well as electromagnetic fields are time dependent.

In the case of some crystal symmetries, one can formulate also the plane-deformation problems (Parton and Kudryavtsev 1988). For instance, in the crystals of hexagonal symmetry (class $6mm$) with x_3 being the 6-order symmetry axis and assuming $u_2 = 0$ as well as the independence of the field quantities on x_2 , i.e. $(\cdot)_{,2} = 0$, we have $\varepsilon_{22} = \varepsilon_{23} = \varepsilon_{12} = E_2 = H_2 = 0$. Then, the constitutive equations (7)-(9) are reduced to the following forms

$$\begin{aligned} \begin{bmatrix} \sigma_{11} \\ \sigma_{33} \\ \sigma_{13} \end{bmatrix} &= \begin{bmatrix} c_{11} & c_{13} & 0 \\ c_{13} & c_{33} & 0 \\ 0 & 0 & c_{44} \end{bmatrix} \begin{bmatrix} \varepsilon_{11} \\ \varepsilon_{33} \\ 2\varepsilon_{13} \end{bmatrix} - \begin{bmatrix} 0 & e_{31} \\ 0 & e_{33} \\ e_{15} & 0 \end{bmatrix} \begin{bmatrix} E_1 \\ E_3 \end{bmatrix} - \begin{bmatrix} 0 & d_{31} \\ 0 & d_{33} \\ d_{15} & 0 \end{bmatrix} \begin{bmatrix} H_1 \\ H_3 \end{bmatrix} = \\ &= \mathbf{C}(\mathbf{x}) \begin{bmatrix} \varepsilon_{11} \\ \varepsilon_{33} \\ 2\varepsilon_{13} \end{bmatrix} - \mathbf{L}(\mathbf{x}) \begin{bmatrix} E_1 \\ E_3 \end{bmatrix} - \mathbf{K}(\mathbf{x}) \begin{bmatrix} H_1 \\ H_3 \end{bmatrix}, \end{aligned} \quad (11)$$

$$\begin{aligned} \begin{bmatrix} D_1 \\ D_3 \end{bmatrix} &= \begin{bmatrix} 0 & 0 & e_{15} \\ e_{31} & e_{33} & 0 \end{bmatrix} \begin{bmatrix} \varepsilon_{11} \\ \varepsilon_{33} \\ 2\varepsilon_{13} \end{bmatrix} + \begin{bmatrix} h_{11} & 0 \\ 0 & h_{33} \end{bmatrix} \begin{bmatrix} E_1 \\ E_3 \end{bmatrix} + \begin{bmatrix} \alpha_{11} & 0 \\ 0 & \alpha_{33} \end{bmatrix} \begin{bmatrix} H_1 \\ H_3 \end{bmatrix} = \\ &= \mathbf{G}(\mathbf{x}) \begin{bmatrix} \varepsilon_{11} \\ \varepsilon_{33} \\ 2\varepsilon_{13} \end{bmatrix} + \mathbf{H}(\mathbf{x}) \begin{bmatrix} E_1 \\ E_3 \end{bmatrix} + \mathbf{A}(\mathbf{x}) \begin{bmatrix} H_1 \\ H_3 \end{bmatrix}, \end{aligned} \quad (12)$$

$$\begin{bmatrix} B_1 \\ B_3 \end{bmatrix} = \begin{bmatrix} 0 & 0 & d_{15} \\ d_{31} & d_{33} & 0 \end{bmatrix} \begin{bmatrix} \varepsilon_{11} \\ \varepsilon_{33} \\ 2\varepsilon_{13} \end{bmatrix} + \begin{bmatrix} \alpha_{11} & 0 \\ 0 & \alpha_{33} \end{bmatrix} \begin{bmatrix} E_1 \\ E_3 \end{bmatrix} + \begin{bmatrix} \gamma_{11} & 0 \\ 0 & \gamma_{33} \end{bmatrix} \begin{bmatrix} H_1 \\ H_3 \end{bmatrix} =$$

$$= \mathbf{R}(\mathbf{x}) \begin{bmatrix} \varepsilon_{11} \\ \varepsilon_{33} \\ 2\varepsilon_{13} \end{bmatrix} + \mathbf{A}(\mathbf{x}) \begin{bmatrix} E_1 \\ E_3 \end{bmatrix} + \mathbf{M}(\mathbf{x}) \begin{bmatrix} H_1 \\ H_3 \end{bmatrix}. \quad (13)$$

It should be noted that $\mathbf{G} = \mathbf{L}^T$ and $\mathbf{R} = \mathbf{K}^T$. Recall that σ_{22} does not influence the governing equations, although it is not vanishing in general, since $\sigma_{22} = c_{12}\varepsilon_{12} + c_{13}\varepsilon_{33} - e_{13}E_3 - d_{13}H_3$.

Let us write the material parameters at the crack-tip vicinity as

$$\begin{aligned} c_{ijkl}(\mathbf{x}) &= c_{ijkl}^0 + \tilde{c}_{ijkl}(\mathbf{x}), & e_{kij}(\mathbf{x}) &= e_{kij}^0 + \tilde{e}_{kij}(\mathbf{x}), & h_{ij}(\mathbf{x}) &= h_{ij}^0 + \tilde{h}_{ij}(\mathbf{x}), \\ d_{kij}(\mathbf{x}) &= d_{kij}^0 + \tilde{d}_{kij}(\mathbf{x}), & \alpha_{jk}(\mathbf{x}) &= \alpha_{jk}^0 + \tilde{\alpha}_{jk}(\mathbf{x}). \end{aligned} \quad (14)$$

Then, the perturbations, denoted by a wave “ \sim ”, behave like $O(r)$, where r is the distance of the observation point \mathbf{x} from the crack-tip.

The governing equations involve the gradients of the stresses, electrical displacements and magnetic inductions, which are given in a medium with continuously varying material properties as

$$\begin{aligned} \sigma_{ij,j} &= c_{ijkl}u_{k,lj} - e_{kij}E_{k,j} - d_{kij}H_{k,j} + c_{ijkl,j}u_{k,l} - e_{kij,j}E_k - d_{kij,j}H_k, \\ D_{j,j} &= e_{jkl}u_{k,lj} + h_{jk}E_{k,j} + \alpha_{jk}H_{k,j} + e_{jkl,j}u_{k,l} + h_{jk,j}E_k + \alpha_{jk,j}H_k, \\ B_{j,j} &= d_{jkl}u_{k,lj} + \alpha_{kj}E_{k,j} + \gamma_{jk}H_{k,j} + d_{jkl,j}u_{k,l} + \alpha_{kj,j}E_k + \gamma_{jk,j}H_k. \end{aligned} \quad (15)$$

For analyzing the asymptotic fields in the crack-tip vicinity, the body forces, volume charges and magnetic induction sources are assumed to be zero. Utilizing eqs. (14) for a quasi-static case, one obtains from (1) and (2)

$$\begin{aligned} c_{ijkl}^0 u_{k,lj} - e_{kij}^0 E_{k,j} - d_{kij}^0 H_{k,j} + \tilde{c}_{ijkl} u_{k,lj} - \tilde{e}_{kij} E_{k,j} - \tilde{d}_{kij} H_{k,j} + c_{ijkl,j} u_{k,l} - e_{kij,j} E_k \\ - d_{kij,j} H_k = 0, \end{aligned} \quad (16)$$

$$\begin{aligned} e_{jkl}^0 u_{k,lj} + h_{jk}^0 E_{k,j} + \alpha_{jk}^0 H_{k,j} + \tilde{e}_{jkl} u_{k,lj} + \tilde{h}_{jk} E_{k,j} + \tilde{\alpha}_{jk} H_{k,j} + e_{jkl,j} u_{k,l} + h_{jk,j} E_k \\ + \alpha_{jk,j} H_k = 0, \end{aligned} \quad (17)$$

$$\begin{aligned} d_{jkl}^0 u_{k,lj} + \alpha_{kj}^0 E_{k,j} + \gamma_{jk}^0 H_{k,j} + \tilde{d}_{jkl} u_{k,lj} + \tilde{\alpha}_{kj} E_{k,j} + \tilde{\gamma}_{jk} H_{k,j} + d_{jkl,j} u_{k,l} + \alpha_{kj,j} E_k \\ + \gamma_{jk,j} H_k = 0. \end{aligned} \quad (18)$$

The method of separation of variables in polar coordinate system is appropriate to solve equations (16)-(18). Our aim is to show that the asymptotic fields in continuously nonhomogeneous medium are the same as in a homogeneous one. For this

purpose we assume that in the near vicinity of the crack-tip, the radial variation of the mechanical displacements is given as $u_i \sim r^\lambda$, where λ is an unspecified positive parameter. From the governing equations (1), the constitutive equation (8) as well as eqs. (2) and (9), one can find directly that the electric and magnetic fields behave like $E_i \sim r^{\lambda-1}$ and $H_i \sim r^{\lambda-1}$, respectively. Then, taking into account the asymptotic behaviour of the material parameters in the continuously non-homogeneous medium in accordance with eq. (14), we can rewrite equations (16)-(18) into the following form

$$c_{ijkl}^0 u_{k,lj} - e_{kij}^0 E_{k,j} - d_{kij}^0 H_{k,j} + O(r^{\lambda-1}) = 0, \quad (19)$$

$$e_{jkl}^0 u_{k,lj} + h_{jk}^0 E_{k,j} + \alpha_{jk}^0 H_{k,j} + O(r^{\lambda-1}) = 0, \quad (20)$$

$$d_{jkl}^0 u_{k,lj} + \alpha_{jk}^0 E_{k,j} + \gamma_{jk}^0 H_{k,j} + O(r^{\lambda-1}) = 0. \quad (21)$$

where the first three terms in each equation are proportional to $r^{\lambda-2}$.

Thus, the leading singularity is determined by the following equations

$$c_{ijkl}^0 u_{k,lj} - e_{kij}^0 E_{k,j} - d_{kij}^0 H_{k,j} = 0, \quad (22)$$

$$e_{jkl}^0 u_{k,lj} + h_{jk}^0 E_{k,j} + \alpha_{jk}^0 H_{k,j} = 0, \quad (23)$$

$$d_{jkl}^0 u_{k,lj} + \alpha_{jk}^0 E_{k,j} + \gamma_{jk}^0 H_{k,j} = 0, \quad (24)$$

which are valid for a homogeneous solid with the material constants given by the crack-tip values of the corresponding material parameters in the considered nonhomogeneous medium. A similar approach has been used by Jin and Noda (1994) to show the dominant crack-tip singularity in a continuously nonhomogeneous solid in linear elasticity. The nature of the stress singularity has precisely the same well-known form applicable to homogeneous materials (Eischen 1987).

For cracks in homogeneous and linear piezoelectric and piezomagnetic solids the asymptotic behaviour of the field quantities has been given by Wang and Mai (2003). In the crack-tip vicinity, the displacements as well as the electric and magnetic potentials show the classical \sqrt{r} asymptotic behaviour. Hence, correspondingly, the stresses, the electrical displacements and magnetic inductions exhibit a $1/\sqrt{r}$ -behaviour, where r is the radial polar coordinate with the origin at the crack-tip. Garcia-Sanchez et al. (2007) extended the approach used in piezoelectricity to magnetoelastoelectricity to obtain the following asymptotic expression for the generalized intensity factors

$$\begin{pmatrix} K_{II} \\ K_I \\ K_D \\ K_B \end{pmatrix} = \sqrt{\frac{\pi}{2r}} [Re(\mathbf{\Pi})^{-1}] \begin{pmatrix} u_1 \\ u_3 \\ \psi \\ \mu \end{pmatrix}, \quad (25)$$

where matrix $\mathbf{\Pi}$ is determined by the material properties (Garcia-Sanchez et al. 2005, 2007) and

$$K_I = \lim_{r \rightarrow 0} \sqrt{2\pi r} \sigma_{33}(r, 0),$$

$$K_{II} = \lim_{r \rightarrow 0} \sqrt{2\pi r} \sigma_{13}(r, 0),$$

$$K_D = \lim_{r \rightarrow 0} \sqrt{2\pi r} D_3(r, 0),$$

$$K_B = \lim_{r \rightarrow 0} \sqrt{2\pi r} B_3(r, 0)$$

are the stress intensity factors (K_I and K_{II}), the electrical displacement intensity factor (K_D), and the magnetic induction intensity factor (K_B), respectively.

3 Evaluation of the intensity factors in FGMs

The gradient of the electromagnetic enthalpy density (6) is given as

$$W_{,m}(\varepsilon_{ij}, E_j, H_j, x_i) = \frac{\partial W}{\partial \varepsilon_{ij}} \frac{\partial \varepsilon_{ij}}{\partial x_m} + \frac{\partial W}{\partial E_j} \frac{\partial E_j}{\partial x_m} + \frac{\partial W}{\partial H_j} \frac{\partial H_j}{\partial x_m} + \left(\frac{\partial W}{\partial x_m} \right)_{\text{expl}}, \quad (26)$$

where the term for the “explicit” derivative of the enthalpy density for non-homogeneous materials can be written as

$$\begin{aligned} \left(\frac{\partial W}{\partial x_m} \right)_{\text{expl}} &= \frac{1}{2} c_{ijkl,m} \varepsilon_{ij} \varepsilon_{kl} - e_{jkl,m} E_j \varepsilon_{kl} - \frac{1}{2} h_{jk,m} E_j E_k - d_{jkl,m} H_j \varepsilon_{kl} - \alpha_{jk,m} H_k E_j - \\ &- \frac{1}{2} \gamma_{jk,m} H_j H_k. \end{aligned} \quad (27)$$

Then, utilizing eqs. (7)-(10), the gradient of the enthalpy density can be rewritten into the form

$$W_{,m} = (\sigma_{ij} u_{i,m})_{,j} - \sigma_{ij,j} u_{i,m} - D_j E_{j,m} - B_j H_{j,m} + (W_{,m})_{\text{expl}}. \quad (28)$$

Bearing in mind of eqs. (3) and (4), one can write the third and the fourth term in eq. (28) as

$$D_j E_{j,m} = -D_j \Psi_{,jm} = D_j E_{m,j} = (D_j E_m)_{,j} - D_{j,j} E_m,$$

$$B_j H_{j,m} = -B_j \mu_{,jm} = B_j H_{m,j} = (B_j H_m)_{,j} - B_{j,j} H_m.$$

Then, in view of the governing equations (1), (2) and (5), the following identity can be obtained

$$(W \delta_{jm} - \sigma_{ij} u_{i,m} + D_j E_m + B_j H_m)_{,j} = (X_i - \rho \ddot{u}_i) u_{i,m} + R E_m + (W_{,m})_{\text{expl}}. \quad (29)$$

Integrating the identity (29) over a regular finite domain Ω with the boundary Γ , we obtain

$$\begin{aligned} \int_{\Gamma} (W \delta_{jm} - \sigma_{ij} u_{i,m} + D_j E_m + B_j H_m) n_j d\Gamma &= \int_{\Omega} (X_i - \rho \ddot{u}_i) u_{i,m} d\Omega + \\ &+ \int_{\Omega} (R E_m) d\Omega + \int_{\Omega} (W_{,m})_{\text{expl}} d\Omega, \end{aligned} \quad (30)$$

where \mathbf{n} is a unit outward normal vector on Γ .

For a linear magneto-electroelastic solid it can be shown that the electromagnetic enthalpy is equal to $W = (\sigma_{ij} \varepsilon_{ij} - D_i E_i - B_i H_i)/2$. The integral identity (30) is valid in a region where no field irregularities prevail. In the presence of a crack, the stresses at the crack-tip are singular and the displacements are discontinuous across both crack-faces. Therefore, a cut-off along the crack with a small circular region in the vicinity of a crack-tip Ω_ε has to be excluded. This small region has a radius ε and is surrounded by Γ_ε as shown in Fig. 1.

The global Cartesian coordinate system is defined in such a way that the principal axes of the material orthotropy are aligned with the global coordinates. All field quantities σ_{ij} , u_i , D_j , E_j and H_j are regular in the region $\Omega - \Omega_\varepsilon$. The contour $\Gamma = \Gamma_0 + \Gamma_c^+ - \Gamma_\varepsilon + \Gamma_c^-$ is a closed integration path in the counter-clockwise direction. The radius ε is considered to be very small and shrunk to zero in the limiting process. The crack-faces Γ_c^+ and Γ_c^- are assumed to be traction-free, with vanishing normal components of the electric displacements and magnetic inductions, i.e., $t_i = \sigma_{ij} n_j = 0$, $D_n = 0$ and $H_n = 0$, and the crack is parallel to the x_1 -axis of the local Cartesian coordinate system. Then, eq. (30) can be written as

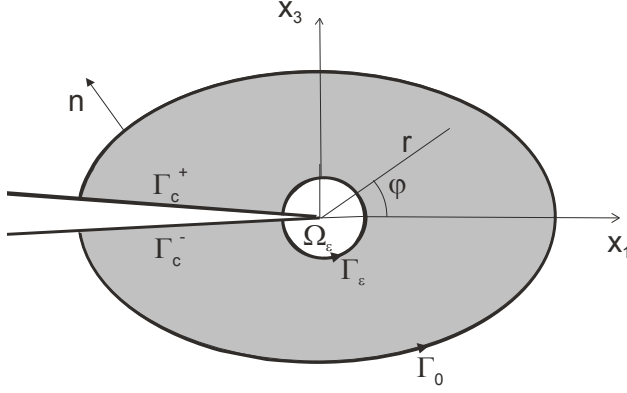


Figure 1: Integration paths and coordinate definitions

$$\begin{aligned}
 & \lim_{\epsilon \rightarrow 0} \int_{\Gamma_\epsilon} (W \delta_{jm} - \sigma_{ij} u_{i,m} + D_j E_m + B_j H_m) n_j d\Gamma \\
 &= \int_{\Gamma_0} (W \delta_{jm} - \sigma_{ij} u_{i,m} + D_j E_m + B_j H_m) n_j d\Gamma + \\
 &+ \int_{\Gamma_c^+} [W^+ - W^-] \delta_{2m} d\Gamma - \lim_{\epsilon \rightarrow 0} \int_{\Omega - \Omega_\epsilon} (X_i - \rho \ddot{u}_i) u_{i,m} d\Omega - \lim_{\epsilon \rightarrow 0} \int_{\Omega - \Omega_\epsilon} R E_m d\Omega - \\
 &- \lim_{\epsilon \rightarrow 0} \int_{\Omega - \Omega_\epsilon} (W, m)_{\text{expl}} d\Omega . \tag{31}
 \end{aligned}$$

The left hand side of eq. (31) is identical to the definition of the J -integral (Wang and Mai 2003, 2004) for $m = 1$ in the linear magnetoelasticity, which has the following form

$$\begin{aligned}
 J_1 &= \int_{\Gamma_0} (W \delta_{j1} - \sigma_{ij} u_{i,1} + D_j E_1 + B_j H_1) n_j d\Gamma - \lim_{\epsilon \rightarrow 0} \int_{\Omega - \Omega_\epsilon} (X_i - \rho \ddot{u}_i) u_{i,1} d\Omega - \\
 &- \lim_{\epsilon \rightarrow 0} \int_{\Omega - \Omega_\epsilon} R E_1 d\Omega - \lim_{\epsilon \rightarrow 0} \int_{\Omega - \Omega_\epsilon} (W, 1)_{\text{expl}} d\Omega . \tag{32}
 \end{aligned}$$

Consider now two independent equilibrium states in an orthotropic functionally graded material. Let the first state be represented by the actual state specified by the prescribed boundary conditions, and the second state (called auxiliary and denoted by superscript 2) is assumed to be a steady-state solution obeying the homogeneous governing equations in the infinite plane. Superposition of the actual and the auxiliary fields leads to another equilibrium state (state “s”) for which the J-integral is given as

$$\begin{aligned}
 J^{(s)} = & \int_{\Gamma_0} \left[W^{(s)} n_1 - (\sigma_{ij} + \sigma_{ij}^{(2)}) n_j (u_{i,1} + u_{i,1}^{(2)}) + (D_j + D_j^{(2)}) n_j (E_1 + E_1^{(2)}) + \right. \\
 & \left. + (B_j + B_j^{(2)}) n_j (H_1 + H_1^{(2)}) \right] d\Gamma - \lim_{\varepsilon \rightarrow 0} \int_{\Omega - \Omega_\varepsilon} (X_i - \rho \ddot{u}_i) (u_{i,1} + u_{i,1}^{(2)}) d\Omega - \\
 & - \lim_{\varepsilon \rightarrow 0} \int_{\Omega - \Omega_\varepsilon} R (E_1 + E_1^{(2)}) d\Omega - \\
 & - \lim_{\varepsilon \rightarrow 0} \int_{\Omega - \Omega_\varepsilon} \left[\frac{1}{2} c_{ijkl,1} (\varepsilon_{ij} + \varepsilon_{ij}^{(2)}) (\varepsilon_{kl} + \varepsilon_{kl}^{(2)}) - e_{jkl,1} (E_j + E_j^{(2)}) (\varepsilon_{kl} + \varepsilon_{kl}^{(2)}) - \right. \\
 & \left. - \frac{1}{2} h_{jk,1} (E_k + E_k^{(2)}) (E_j + E_j^{(2)}) - d_{jkl,1} (H_j + H_j^{(2)}) (\varepsilon_{kl} + \varepsilon_{kl}^{(2)}) - \right. \\
 & \left. - \alpha_{jk,1} (H_k + H_k^{(2)}) (E_j + E_j^{(2)}) - \frac{1}{2} \gamma_{jk,1} (H_k + H_k^{(2)}) (H_j + H_j^{(2)}) \right] d\Omega,
 \end{aligned} \tag{33}$$

where

$$\begin{aligned}
 W^{(s)} = & \frac{1}{2} \left[(\sigma_{ij} + \sigma_{ij}^{(2)}) (\varepsilon_{ij} + \varepsilon_{ij}^{(2)}) - (D_j + D_j^{(2)}) (E_j + E_j^{(2)}) - (B_j + B_j^{(2)}) (H_j + H_j^{(2)}) \right].
 \end{aligned}$$

The J-integral (33) can be conveniently decomposed into

$$J^{(s)} = J + J^{(2)} + M, \tag{34}$$

where

$$\begin{aligned}
 J^{(2)} &= \int_{\Gamma_0} \left[W^{(2)} n_1 - \sigma_{ij}^{(2)} n_j u_{i,1}^{(2)} - D_j^{(2)} n_j E_1^{(2)} \right] d\Gamma - \\
 &- \lim_{\varepsilon \rightarrow 0} \int_{\Omega - \Omega_\varepsilon} \left[\frac{1}{2} c_{ijkl,1} \varepsilon_{ij}^{(2)} \varepsilon_{kl}^{(2)} - e_{jkl,1} E_j^{(2)} \varepsilon_{kl}^{(2)} - \right. \\
 &\left. - \frac{1}{2} h_{jk,1} E_k^{(2)} E_j^{(2)} - d_{jkl,1} H_j^{(2)} \varepsilon_{kl}^{(2)} - \alpha_{jk,1} H_k^{(2)} E_j^{(2)} - \frac{1}{2} \gamma_{jk,1} H_k^{(2)} H_j^{(2)} \right] d\Omega, \quad (35)
 \end{aligned}$$

with

$$W^{(2)} = \frac{1}{2} \left[\sigma_{ij}^{(2)} \varepsilon_{ij}^{(2)} - D_j^{(2)} E_j^{(2)} - B_j^{(2)} H_j^{(2)} \right].$$

The interaction integral M is then given by

$$\begin{aligned}
 M &= \int_{\Gamma_0} \left[W^{(1,2)} n_1 - (\sigma_{ij} n_j u_{i,1}^{(2)} + \sigma_{ij}^{(2)} n_j u_{i,1}) + D_j n_j E_1^{(2)} + \right. \\
 &\left. + D_j^{(2)} n_j E_1 + B_j n_j H_1^{(2)} + B_j^{(2)} n_j H_1 \right] d\Gamma - \\
 &- \lim_{\varepsilon \rightarrow 0} \int_{\Omega - \Omega_\varepsilon} (X_i - \rho \ddot{u}_i) u_{i,1}^{(2)} d\Omega - \lim_{\varepsilon \rightarrow 0} \int_{\Omega - \Omega_\varepsilon} R E_1^{(2)} d\Omega - \\
 &- \lim_{\varepsilon \rightarrow 0} \int_{\Omega - \Omega_\varepsilon} \left[\frac{1}{2} c_{ijkl,1} \left(\varepsilon_{ij} \varepsilon_{kl}^{(2)} + \varepsilon_{ij}^{(2)} \varepsilon_{kl} \right) - e_{jkl,1} \left(E_j \varepsilon_{kl}^{(2)} + E_j^{(2)} \varepsilon_{kl} \right) - \right. \\
 &\left. - \frac{1}{2} h_{jk,1} \left(E_k E_j^{(2)} + E_k^{(2)} E_j \right) - d_{jkl,1} \left(H_j \varepsilon_{kl}^{(2)} + H_j^{(2)} \varepsilon_{kl} \right) - \right. \\
 &\left. - \alpha_{jk,1} \left(H_k E_j^{(2)} + H_k^{(2)} E_j \right) - \frac{1}{2} \gamma_{jk,1} \left(H_k H_j^{(2)} + H_k^{(2)} H_j \right) \right] d\Omega. \quad (36)
 \end{aligned}$$

The magnetoelastoelectric J - integral can be expressed in terms of the SIFs, the electrical displacement intensity factor (EDIF) and the magnetic induction intensity factor (MIIF) as (Rao and Kuna 2008b)

$$J = \frac{1}{2} K_L K_N Y_{LN}, \quad (37)$$

where Y_{LN} is the generalized Irwin matrix with a size (5x5) (Rao and Kuna 2008b). For 2-D problems one can write

$$J = K_{II}^2 Y_{11}/2 + K_I^2 Y_{22}/2 + K_D^2 Y_{44}/2 + K_B^2 Y_{55}/2 + K_I K_{II} Y_{12} + K_I K_D Y_{24} + K_I K_B Y_{25} + K_{II} K_D Y_{14} + K_{II} K_B Y_{15} + K_D K_B Y_{45}. \quad (38)$$

The J-integral for auxiliary fields and the M-integral are given as

$$J^{(2)} = K_{II}^{(2)2} Y_{11}/2 + K_I^{(2)2} Y_{22}/2 + K_D^{(2)2} Y_{44}/2 + K_B^{(2)2} Y_{55}/2 + K_I^{(2)} K_{II}^{(2)} Y_{12} + K_I^{(2)} K_D^{(2)} Y_{24} + K_I^{(2)} K_B^{(2)} Y_{25} + K_{II}^{(2)} K_D^{(2)} Y_{14} + K_{II}^{(2)} K_B^{(2)} Y_{15} + K_D^{(2)} K_B^{(2)} Y_{45},$$

$$M = K_{II} K_{II}^{(2)} Y_{11} + K_I K_I^{(2)} Y_{22} + K_D K_D^{(2)} Y_{44} + K_B K_B^{(2)} Y_{55} + (K_I K_{II}^{(2)} + K_{II} K_I^{(2)}) Y_{12} + (K_I K_D^{(2)} + K_D K_I^{(2)}) Y_{24} + (K_I K_B^{(2)} + K_B K_I^{(2)}) Y_{25} + (K_{II} K_D^{(2)} + K_D K_{II}^{(2)}) Y_{14} + (K_{II} K_B^{(2)} + K_B K_{II}^{(2)}) Y_{15} + (K_D K_B^{(2)} + K_B K_D^{(2)}) Y_{45}. \quad (39)$$

The individual intensity factors (SIFs, EDIF, MIIF) are evaluated by solving the system of linear algebraic equations obtained from eq. (39) by choosing appropriate auxiliary states. If $K_I^{(2)} = 1$ and $K_{II}^{(2)} = K_D^{(2)} = K_B^{(2)} = 0$ one obtains

$$M^I = K_I Y_{22} + K_{II} Y_{12} + K_D Y_{24} + K_B Y_{25}. \quad (40)$$

Similarly, one obtains 3 additional equations as

$$M^{II} = K_I Y_{12} + K_{II} Y_{11} + K_D Y_{14} + K_B Y_{15},$$

$$M^D = K_I Y_{24} + K_{II} Y_{14} + K_D Y_{44} + K_B Y_{45},$$

$$M^B = K_I Y_{25} + K_{II} Y_{15} + K_D Y_{45} + K_B Y_{55} \quad (41)$$

resulting from eq. (39) by taking $K_{II}^{(2)} = 1$, $K_I^{(2)} = K_D^{(2)} = K_B^{(2)} = 0$ for M^{II} , $K_D^{(2)} = 1$, $K_I^{(2)} = K_{II}^{(2)} = K_B^{(2)} = 0$ for M^D , and $K_B^{(2)} = 1$, $K_I^{(2)} = K_{II}^{(2)} = K_D^{(2)} = 0$ for M^B , respectively. The values M^I , M^{II} , M^D and M^B are computed numerically by using eq. (36) with an adequate choice of the auxiliary solutions.

The interaction integral expression M given in eq. (36) has a contour-domain integral character. Only the terms with the acceleration, the body forces, the volume density of free charges and magnetic induction sources and the gradients of the material parameters appear in the domain integrals. These terms are vanishing for a steady-state and homogeneous material case provided that body sources are absent. Then, the principal character of the M integral expression is given by the contour integral. Therefore, the present method is very convenient for computational schemes where the accuracy of computed quantities on a contour is high, like in the BEM or present meshless method. The domain integral form for the interaction integral given by Rao and Kuna (2008b) is more convenient for the FEM, because the results are more accurate in the integration points than at interelement contours. The volume integration is easier in the FEM concept.

4 Local integral equations for 2-D problems

The following essential and natural boundary conditions are assumed for the mechanical field

$$u_i(\mathbf{x}, \tau) = \tilde{u}_i(\mathbf{x}, \tau), \text{ on } \Gamma_u,$$

$$t_i(\mathbf{x}, \tau) = \sigma_{ij} n_j = \tilde{t}_i(\mathbf{x}, \tau), \text{ on } \Gamma_t, \Gamma = \Gamma_u \cup \Gamma_t.$$

We assume for the electrical field

$$\psi(\mathbf{x}, \tau) = \tilde{\psi}(\mathbf{x}, \tau), \text{ on } \Gamma_p,$$

$$n_i(\mathbf{x}) D_i(\mathbf{x}, \tau) \equiv Q(\mathbf{x}, \tau) = \tilde{Q}(\mathbf{x}, \tau), \text{ on } \Gamma_q, \Gamma = \Gamma_p \cup \Gamma_q,$$

and for the magnetic field

$$\mu(\mathbf{x}, \tau) = \tilde{\mu}(\mathbf{x}, \tau), \text{ on } \Gamma_a,$$

$$n_i(\mathbf{x}) B_i(\mathbf{x}, \tau) \equiv S(\mathbf{x}, \tau) = \tilde{S}(\mathbf{x}, \tau), \text{ on } \Gamma_b, \Gamma = \Gamma_a \cup \Gamma_b,$$

where Γ_u is the part of the global boundary Γ with prescribed displacements, while on Γ_t , Γ_p , Γ_q , Γ_a , and Γ_b the traction vector, the electric potential, the normal component of the electric displacement vector, the magnetic potential and the normal component of the magnetic induction vector are prescribed, respectively. Recall that $\tilde{Q}(\mathbf{x}, \tau)$ can be considered approximately as the surface density of free charges, provided that the permittivity of the solid is much larger than that of the surrounding medium (vacuum).

The initial conditions for the mechanical displacements are assumed as

$$u_i(\mathbf{x}, \tau)|_{\tau=0} = u_i(\mathbf{x}, 0) \text{ and } \dot{u}_i(\mathbf{x}, \tau)|_{\tau=0} = \dot{u}_i(\mathbf{x}, 0) \text{ in } \Omega.$$

Recently, the authors have derived the local integral equations to solve a general boundary value problem in magneto-electro-elasticity [Sladek et al., 2008]. The integral equations have the following form

$$\int_{L_s + \Gamma_{su}} t_i(\mathbf{x}, \tau) d\Gamma - \int_{\Omega_s} \rho \ddot{u}_i(\mathbf{x}, \tau) d\Omega = - \int_{\Gamma_{st}} \tilde{t}_i(\mathbf{x}, \tau) d\Gamma - \int_{\Omega_s} X_i(\mathbf{x}, \tau) d\Omega, \quad (42)$$

$$\int_{L_s + \Gamma_{sp}} Q(\mathbf{x}, \tau) d\Gamma = - \int_{\Gamma_{sq}} \tilde{Q}(\mathbf{x}, \tau) d\Gamma + \int_{\Omega_s} R(\mathbf{x}, \tau) d\Omega, \quad (43)$$

$$\int_{L_s + \Gamma_{sa}} S(\mathbf{x}, \tau) d\Gamma = - \int_{\Gamma_{sb}} \tilde{S}(\mathbf{x}, \tau) d\Gamma, \quad (44)$$

where

$$Q(\mathbf{x}, \tau) = D_j(\mathbf{x}, \tau) n_j(\mathbf{x}) = [e_{jkl} u_{k,l}(\mathbf{x}, \tau) - h_{jk} \psi_{,k}(\mathbf{x}, \tau) - \alpha_{jk} \mu_{,k}(\mathbf{x}, \tau)] n_j.$$

$$S(\mathbf{x}, \tau) = B_j(\mathbf{x}, \tau) n_j(\mathbf{x}) = [d_{jkl} u_{k,l}(\mathbf{x}, \tau) - \alpha_{kj} \psi_{,k}(\mathbf{x}, \tau) - \gamma_{jk} \mu_{,k}(\mathbf{x}, \tau)] n_j.$$

The trial functions can be approximated by the moving least squares (MLS) method using a number of nodes spreading over the analyzed domain. According to the MLS (Belytschko et al. 1996) method, the approximation of the mechanical displacements, and the electric and magnetic potentials can be written as

$$\mathbf{u}^h(\mathbf{x}, \tau) = \mathbf{\Phi}^T(\mathbf{x}) \cdot \hat{\mathbf{u}} = \sum_{a=1}^n \phi^a(\mathbf{x}) \hat{\mathbf{u}}^a(\tau),$$

$$\psi^h(\mathbf{x}, \tau) = \sum_{a=1}^n \phi^a(\mathbf{x}) \hat{\psi}^a(\tau),$$

$$\mu^h(\mathbf{x}, \tau) = \sum_{a=1}^n \phi^a(\mathbf{x}) \hat{\mu}^a(\tau), \quad (45)$$

where the nodal values $\hat{\mathbf{u}}^a(\tau) = (\hat{u}_1^a(\tau), \hat{u}_3^a(\tau))^T$, $\hat{\psi}^a(\tau)$ and $\hat{\mu}^a(\tau)$ are fictitious parameters for the displacements, the electric and magnetic potentials, respectively, and $\phi^a(\mathbf{x})$ is the shape function associated with the node a . The number of nodes n used for the approximation is determined by the weight function $w^a(\mathbf{x})$. A 4th order spline-type weight function is applied in the present work.

Then, the traction vector $t_i(\mathbf{x}, \tau)$ at a boundary point $\mathbf{x} \in \partial\Omega_s$ is approximated in terms of the same nodal values $\hat{\mathbf{u}}^a(\tau)$ as

$$\mathbf{t}^h(\mathbf{x}, \tau) = \mathbf{N}(\mathbf{x})\mathbf{C}(\mathbf{x}) \sum_{a=1}^n \mathbf{Z}^a(\mathbf{x})\hat{\mathbf{u}}^a(\tau) + \mathbf{N}(\mathbf{x})\mathbf{L}(\mathbf{x}) \sum_{a=1}^n \mathbf{P}^a(\mathbf{x})\hat{\psi}^a(\tau) + \mathbf{N}(\mathbf{x})\mathbf{K}(\mathbf{x}) \sum_{a=1}^n \mathbf{P}^a(\mathbf{x})\hat{\mu}^a(\tau), \quad (46)$$

where the matrices $\mathbf{C}(\mathbf{x})$, $\mathbf{L}(\mathbf{x})$ and $\mathbf{K}(\mathbf{x})$ are defined in eq. (11), the matrix $\mathbf{N}(\mathbf{x})$ is related to the normal vector $\mathbf{n}(\mathbf{x})$ on $\partial\Omega_s$ by

$$\mathbf{N}(\mathbf{x}) = \begin{bmatrix} n_1 & 0 & n_3 \\ 0 & n_3 & n_1 \end{bmatrix},$$

and finally, the matrices \mathbf{Z}^a and \mathbf{P}^a are represented by the gradients of the shape functions as

$$\mathbf{Z}^a(\mathbf{x}) = \begin{bmatrix} \phi_{,1}^a & 0 \\ 0 & \phi_{,3}^a \\ \phi_{,3}^a & \phi_{,1}^a \end{bmatrix}, \quad \mathbf{P}^a(\mathbf{x}) = \begin{bmatrix} \phi_{,1}^a \\ \phi_{,3}^a \end{bmatrix}.$$

Similarly the normal component of the electric displacement vector $Q(\mathbf{x}, \tau)$ can be approximated by

$$Q^h(\mathbf{x}, \tau) = \mathbf{N}_1(\mathbf{x})\mathbf{G}(\mathbf{x}) \sum_{a=1}^n \mathbf{Z}^a(\mathbf{x})\hat{\mathbf{u}}^a(\tau) - \mathbf{N}_1(\mathbf{x})\mathbf{H}(\mathbf{x}) \sum_{a=1}^n \mathbf{P}^a(\mathbf{x})\hat{\psi}^a(\tau) - \mathbf{N}_1(\mathbf{x})\mathbf{A}(\mathbf{x}) \sum_{a=1}^n \mathbf{P}^a(\mathbf{x})\hat{\mu}^a(\tau), \quad (47)$$

where the matrices $\mathbf{G}(\mathbf{x})$, $\mathbf{H}(\mathbf{x})$ and $\mathbf{A}(\mathbf{x})$ are defined in eq. (12) and

$$\mathbf{N}_1(\mathbf{x}) = \begin{bmatrix} n_1 & n_3 \end{bmatrix}.$$

Eventually, the magnetic flux $S(\mathbf{x}, \tau)$ is approximated by

$$S^h(\mathbf{x}, \tau) = \mathbf{N}_1(\mathbf{x})\mathbf{R}(\mathbf{x}) \sum_{a=1}^n \mathbf{Z}^a(\mathbf{x})\hat{\mathbf{u}}^a(\tau) - \mathbf{N}_1(\mathbf{x})\mathbf{A}(\mathbf{x}) \sum_{a=1}^n \mathbf{P}^a(\mathbf{x})\hat{\psi}^a(\tau) - \mathbf{N}_1(\mathbf{x})\mathbf{M}(\mathbf{x}) \sum_{a=1}^n \mathbf{P}^a(\mathbf{x})\hat{\mu}^a(\tau), \quad (48)$$

with the matrices $\mathbf{R}(\mathbf{x})$, $\mathbf{A}(\mathbf{x})$ and $\mathbf{M}(\mathbf{x})$ being defined in eq. (13).

Furthermore, in view of the MLS-approximations (46)-(48) for the unknown quantities in the local boundary-domain integral equations (42)-(44), we obtain their discretized forms as

$$\begin{aligned} & \sum_{a=1}^n \left[\left(\int_{L_s + \Gamma_{st}} \mathbf{N}(\mathbf{x})\mathbf{C}(\mathbf{x})\mathbf{Z}^a(\mathbf{x})d\Gamma \right) \hat{\mathbf{u}}^a(\tau) - \left(\int_{\Omega_s} \rho(\mathbf{x})\phi^a d\Omega \right) \ddot{\mathbf{u}}^a(\tau) \right] + \\ & + \sum_{a=1}^n \left(\int_{L_s + \Gamma_{st}} \mathbf{N}(\mathbf{x})\mathbf{L}(\mathbf{x})\mathbf{P}^a(\mathbf{x})d\Gamma \right) \hat{\psi}^a(\tau) + \sum_{a=1}^n \left(\int_{L_s + \Gamma_{st}} \mathbf{N}(\mathbf{x})\mathbf{K}(\mathbf{x})\mathbf{P}^a(\mathbf{x})d\Gamma \right) \hat{\mu}^a(\tau) = \\ & = - \int_{\Gamma_{st}} \tilde{\mathbf{t}}(\mathbf{x}, \tau)d\Gamma - \int_{\Omega_s} \mathbf{X}(\mathbf{x}, \tau)d\Omega, \end{aligned} \quad (49)$$

$$\begin{aligned} & \sum_{a=1}^n \left(\int_{L_s + \Gamma_{sq}} \mathbf{N}_1(\mathbf{x})\mathbf{G}(\mathbf{x})\mathbf{Z}^a(\mathbf{x})d\Gamma \right) \hat{\mathbf{u}}^a(\tau) - \sum_{a=1}^n \left(\int_{L_s + \Gamma_{sq}} \mathbf{N}_1(\mathbf{x})\mathbf{H}(\mathbf{x})\mathbf{P}^a(\mathbf{x})d\Gamma \right) \hat{\psi}^a(\tau) - \\ & - \sum_{a=1}^n \left(\int_{L_s + \Gamma_{sq}} \mathbf{N}_1(\mathbf{x})\mathbf{A}(\mathbf{x})\mathbf{P}^a(\mathbf{x})d\Gamma \right) \hat{\mu}^a(\tau) = - \int_{\Gamma_{sq}} \tilde{\mathbf{Q}}(\mathbf{x}, \tau)d\Gamma + \int_{\Omega_s} \mathbf{R}(\mathbf{x}, \tau)d\Omega, \end{aligned} \quad (50)$$

$$\begin{aligned} & \sum_{a=1}^n \left(\int_{L_s + \Gamma_{sb}} \mathbf{N}_1(\mathbf{x})\mathbf{R}(\mathbf{x})\mathbf{Z}^a(\mathbf{x})d\Gamma \right) \hat{\mathbf{u}}^a(\tau) - \sum_{a=1}^n \left(\int_{L_s + \Gamma_{sb}} \mathbf{N}_1(\mathbf{x})\mathbf{A}(\mathbf{x})\mathbf{P}^a(\mathbf{x})d\Gamma \right) \hat{\psi}^a(\tau) - \\ & - \sum_{a=1}^n \left(\int_{L_s + \Gamma_{sb}} \mathbf{N}_1(\mathbf{x})\mathbf{M}(\mathbf{x})\mathbf{P}^a(\mathbf{x})d\Gamma \right) \hat{\mu}^a(\tau) = - \int_{\Gamma_{sb}} \tilde{\mathbf{S}}(\mathbf{x}, \tau)d\Gamma, \end{aligned} \quad (51)$$

which are considered on the subdomains adjacent to the interior nodes as well as to the boundary nodes on Γ_{st} , Γ_{sq} and Γ_{sb} .

The discretized local boundary-domain integral equations represent a complete system of ordinary differential equations, and it can be rearranged in such a way that all known quantities are on the r.h.s. Thus, in matrix form the system becomes

$$\mathbf{F}\ddot{\mathbf{x}} + \Lambda\mathbf{x} = \mathbf{Y}. \quad (52)$$

There are many time integration procedures for solution of this system of ordinary differential equations. In the present work, the Houbolt method is applied. In the Houbolt finite-difference scheme (Houbolt 1950), the ‘‘acceleration’’ $\ddot{\mathbf{x}}$ is approximated by

$$\ddot{\mathbf{x}}_{\tau+\Delta\tau} = \frac{2\mathbf{x}_{\tau+\Delta\tau} - 5\mathbf{x}_{\tau} + 4\mathbf{x}_{\tau-\Delta\tau} - \mathbf{x}_{\tau-2\Delta\tau}}{\Delta\tau^2}, \quad (53)$$

where $\Delta\tau$ is the time-step.

Substituting eqs. (53) into eq. (52), we get the following system of linear algebraic equations for the unknowns $\mathbf{x}_{\tau+\Delta\tau}$

$$\left[\frac{2}{\Delta\tau^2}\mathbf{F} + \Lambda \right] \mathbf{x}_{\tau+\Delta\tau} = \frac{1}{\Delta\tau^2}5\mathbf{F}\mathbf{x}_{\tau} + \mathbf{F}\frac{1}{\Delta\tau^2} \{-4\mathbf{x}_{\tau-\Delta\tau} + \mathbf{x}_{\tau-2\Delta\tau}\} + \mathbf{Y}. \quad (54)$$

The value of the time-step has to be appropriately selected with respect to material parameters (elastic wave velocities) and time dependence of the boundary conditions. Computed quantities from the system of algebraic equations (54) are used for evaluation of the interaction integral M and for intensity factors.

5 Numerical examples

5.1 A central crack in a finite strip

In the first example, a straight central crack in a finite magnetoelastic strip under a uniform pure mechanical and/or electro-magnetic loading is analyzed. The mechanical load $\sigma_0 = 1Pa$ or the magnetic induction load $B_0 = 1Vs/m^2$ is applied on the top side of the strip, respectively, in the static analysis. Each of the loads can open the crack and even cause its propagation. Due to the bi-axial symmetry of the problem only a quarter of the cracked strip is modeled (Fig. 2). The poling direction of the material coincides with the x_3 coordinate direction. The cracked strip is described by the geometrical parameters: $a = 0.5m$, $a/w = 0.4$ and $h/w = 1.2$. The mechanical displacements, the electrical and magnetic potentials in the

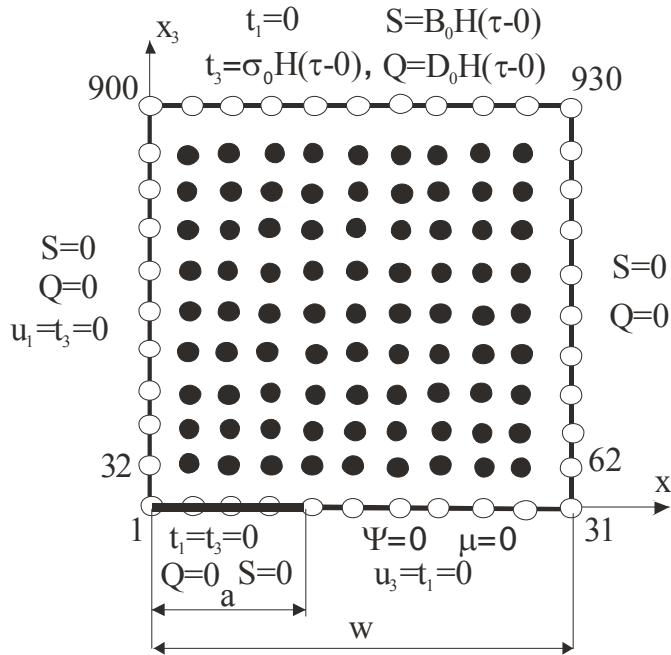


Figure 2: A central crack in a finite magneto-electroelastic strip

finite strip are approximated by using 930 (31x30) equidistantly distributed nodes. The local subdomains are selected to be circular with a radius $r_{loc} = 0.028m$.

To test the accuracy of the present method, homogeneous material properties are first considered. The material parameters corresponding to the BaTiO₃ - CoFe₂O₄ composite are given by Li (2000)

$$c_{11} = 22.6 \times 10^{10} Nm^{-2}, \quad c_{13} = 12.4 \times 10^{10} Nm^{-2},$$

$$c_{33} = 21.6 \times 10^{10} Nm^{-2}, \quad c_{66} = 4.4 \times 10^{10} Nm^{-2},$$

$$e_{15} = 5.8 Cm^{-2}, \quad e_{31} = -2.2 Cm^{-2}, \quad e_{33} = 9.3 Cm^{-2},$$

$$h_{11} = 5.64 \times 10^{-9} C^2/Nm^2, \quad h_{33} = 6.35 \times 10^{-9} C^2/Nm^2,$$

$$d_{15} = 275.0N/Am, \quad d_{21} = 290.2N/Am, \quad d_{22} = 350.0N/Am,$$

$$\alpha_{11} = 5.367 \times 10^{-12}Ns/VC, \quad \alpha_{33} = 2737.5 \times 10^{-12}Ns/VC,$$

$$\gamma_{11} = 297.0 \times 10^{-6}Ns^2C^{-2}, \quad \gamma_{33} = 83.5 \times 10^{-6}Ns^2C^{-2}, \quad \rho = 5500kg/m^3. \quad (55)$$

If a crack in magnetoelastic solids is investigated, an important question is how the medium inside the crack is modeled. Depending on the ratio between the dielectric permittivity and/or magnetic permeability of the medium inside the crack and that of the cracked solid, two extreme cases can be considered. In the first extreme case, the crack is not visible for the electric and/or magnetic field if the permittivity of the medium inside the crack is significantly larger than that of the analyzed solid. In such a case, the potentials on both crack-surfaces are the same, and thus one has the so-called electrically and magnetically permeable boundary conditions on the crack-faces, i.e.,

$$\psi^+ = \psi^-, \quad \mu^+ = \mu^-,$$

$$D_n^+ = D_n^-, \quad B_n^+ = B_n^-. \quad (56)$$

In the second extreme case, the permittivity of the medium inside the crack is vanishing. Then, jumps in the electric and magnetic potentials occur, and the normal electrical displacement and the magnetic induction on both crack-faces are vanishing, i.e.,

$$\Delta\psi = \psi^+ - \psi^- \neq 0, \quad \Delta\mu = \mu^+ - \mu^- \neq 0,$$

$$D_n^+ = D_n^- = 0, \quad B_n^+ = B_n^- = 0. \quad (57)$$

This case corresponds to the so-called impermeable boundary conditions and they are shown in Fig. 2. Though the crack opening displacement under static loading conditions is slightly larger for permeable boundary conditions under a pure mechanical load than that for the impermeable ones, the mode-I stress intensity factor (SIF) under a pure mechanical load is the same for both boundary conditions, i.e., $K_I^{stat} = 1.4Pa \cdot m^{1/2}$. The boundary element method (BEM) is used here for comparative purposes to test the present MLPG method. The BEM results are obtained using 104 linear elements on the external boundary and 20 elements on

the crack-face. At the crack-tips, the square-root shape functions are implemented to describe the local behaviour of the displacements, the electric and magnetic potentials properly. Both polynomial and enriched basis functions are applied in our MLPG computations. However, the selection of the enriched basis functions has no significant accuracy improvement of the mode-I SIF. This is due to the application of the interaction integral method for the evaluation of the mode-I SIF. If the asymptotic expansion equations have been applied for the evaluation of the mode-I SIF, slight differences have been observed (Sladek et al. 2008). In our case the integration contour for the computation of the M integral is sufficiently far from the crack-tip and the influence of the enriched basis functions is thus vanishing. The integration contour has a rectangular shape composed of 3 straight lines: two vertical lines with $x_1 = 0.917m$ and $x_1 = 0.$, the horizontal line with $x_3 = 0.917m$. The contour is divided into 66 segments with a uniform length for the evaluation of the contour integral and the domain is discretized by 441 square elements with a side length equal to the distance between two nodes used in the MLPG analysis. It is interesting to note that a pure mechanical loading induces finite values of the electrical and magnetic potentials on both crack-faces, but the electrical displacement intensity factor (EDIF) and/or the magnetic induction intensity factor (MIIF) do not appear. It means that the crack displacement u_3 and both the electrical and magnetic potentials ψ_m and μ_m are coupled mutually, but the mode-I SIF and both EDIF and MIIF in this case are uncoupled. The EDIF and MIIF are vanishing for a pure mechanical load under a quasi-static assumption.

Next, the strip is subjected to an impact load with the Heaviside time variation and the amplitude $\sigma_0 = 1Pa$ for a pure mechanical load or $B_0 = 1Vs/m^2$ for a pure magnetic induction load, respectively. Both impermeable and permeable boundary conditions on the crack-faces are considered. The time variation of the normalized mode-I SIF is given in Fig. 3. Both extreme crack-face boundary conditions have a vanishing influence on the mode-I SIF for a pure mechanical load. The dynamic value of the mode-I SIF is approximately doubled as compared to the corresponding static one.

In Figs. 4 and 5, we present the time variations of the EDIF and MIIF under a pure mechanical load. On contrary to the static case, a finite value for both intensity factors is observed here. From the Maxwell's equations, it is known that the velocity of electromagnetic waves is equal to the speed of light, which is much larger than the velocity of elastic waves. Hence, the use of quasi-static approximation in the governing equations is justified for the interaction of electro-magnetic and mechanical fields. The response of the electro-magnetic fields is immediate, while that of the elastic one takes some finite time because of the finite velocity of elastic waves. On the other hand, in a static case, the response of both the mechanical (strains

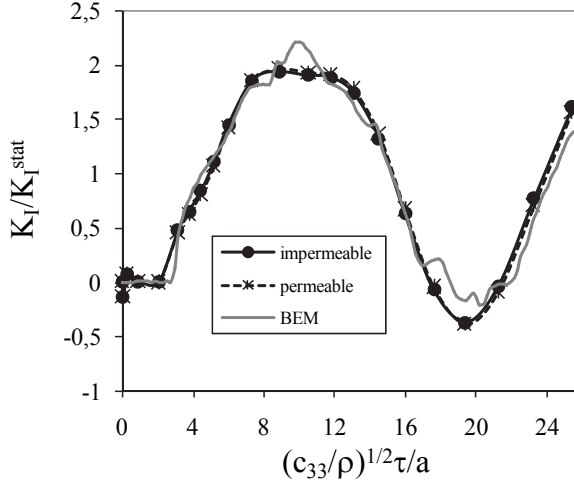


Figure 3: Normalized mode-I stress intensity factor for a central crack in a strip under a pure mechanical load $\sigma_0 H(\tau - 0)$

and stresses) and the electro-magnetic fields is immediate. In the dynamic case the stress evolution is affected by the inertia forces and the electro-magnetic fields follow the time evolution of the mechanical field due to the immediate response within their quasi-static approximation.

For normalized electrical displacement and magnetic induction intensity factors we have used the normalization parameters $\Lambda_d = e_{33}/h_{33}$ and $\Lambda_b = d_{33}/\gamma_{33}$, respectively. The EDIF and MIIF are higher for permeable electro-magnetic crack-face boundary conditions than that for the impermeable ones.

Figure 6 presents the normalized mode-I stress and electrical displacement intensity factors for a pure magnetic induction impact load. The static magnetic induction intensity factor $K_B^{stat} = 1.4 \text{Vs m}^{-3/2}$ is equal to the static mode-I SIF for a pure mechanical load due to their decoupling. Both mode-I SIF and EDIF are oscillating around their mean value with vanishing amplitudes. Since the dynamic SIF and EDIF exceed their static values, they have to be considered in the design of magneto-electroelastic components and devices where transient processes are expected. On the other hand, the temporal variation of the MIIF is slightly oscillating around its static value K_B^{stat} , because the applied magnetic load is only slightly influenced due to the weak magneto-elastic coupling. Nevertheless, there is a finite elastic response and consequently the response of the electric field is influenced by the

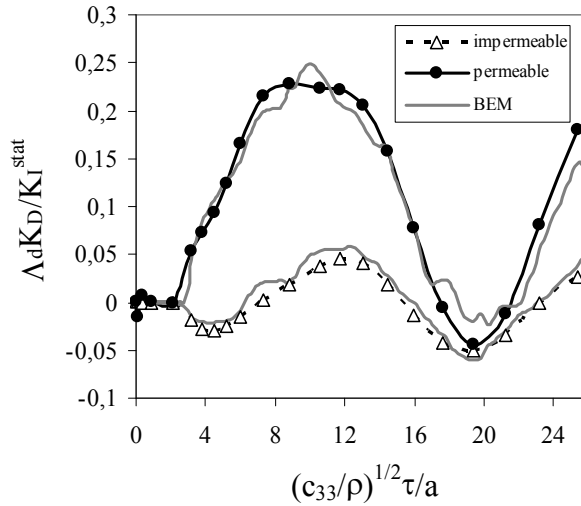


Figure 4: Normalized electrical displacement intensity factors (EDIF) for a central crack in a strip under a pure mechanical load $\sigma_0 H(\tau - 0)$

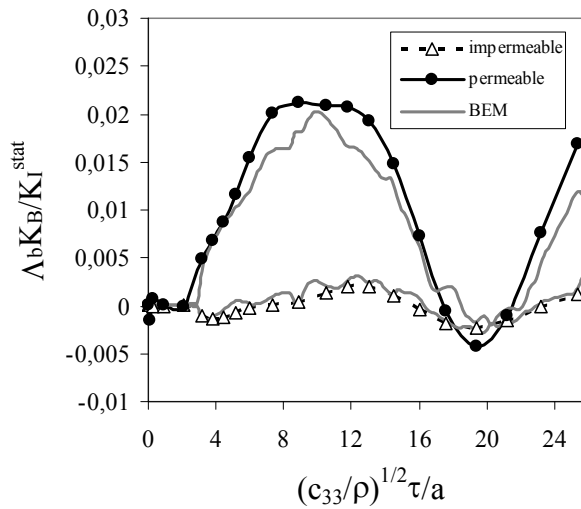


Figure 5: Normalized magnetic induction intensity factors (MIIF) for a central crack in a strip under a pure mechanical load $\sigma_0 H(\tau - 0)$

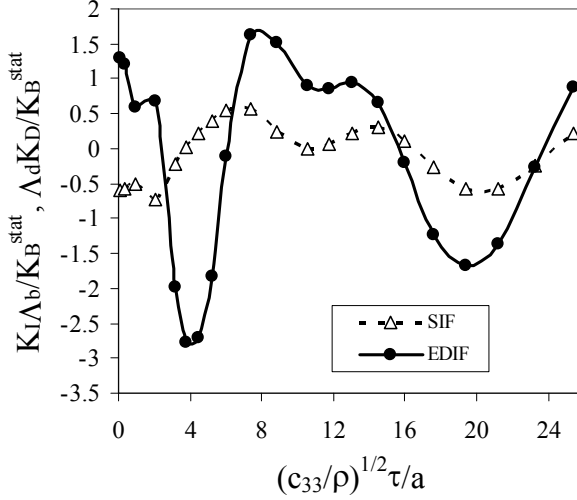


Figure 6: Normalized mode-I stress and electrical displacement intensity factors for a central crack in a strip under a pure magnetic induction load $B_0H(\tau = 0)$

inertial effect of the elastic field due to the electro-elastic coupling.

5.2 An edge crack in a finite strip

Next, an edge crack in a finite magneto-electroelastic strip is analyzed. The geometry of the strip is given in Fig. 7 with the following values: $a = 0.5$, $a/w = 0.4$ and $h/w = 1.2$. Due to the symmetry of the problem with respect to the x_1 -axis, only a half of the strip is modeled. We have used again 930 equidistantly distributed nodes for the MLS approximation of the physical fields. On the top of the strip either a uniform tension σ_0 or a uniform magnetic induction B_0 is applied. Firstly, the static loading case is investigated. The functionally graded material properties in the x_1 -direction are considered. An exponential variation of the elastic, piezoelectric, dielectric, paramagnetic, electromagnetic and magnetic permeability coefficients are assumed as

$$f_{ij}(\mathbf{x}) = f_{ij0} \exp(\gamma_f x_1), \tag{58}$$

where the symbol f_{ij} is commonly used for particular material coefficients and f_{ij0} corresponds to the material parameters used in the previous example. It should be noted here that different gradient parameters γ_f can be used for particular material coefficients.

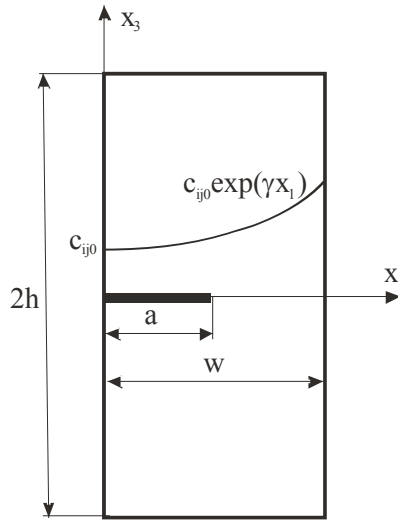


Figure 7: An edge crack in a finite strip with functionally graded material properties in x_1 -direction

For simplicity, we have used the same gradient parameters for all material coefficients with the value $\gamma = 2$ in the numerical calculations. Then, all material parameters at the crack-tip are $e^1 = 2.718$ times larger than that ones in the corresponding homogeneous material. The normalized mode-I stress intensity factors for homogeneous and nonhomogeneous cracked strips take the values $f_I = K_I / \sigma_0 \sqrt{\pi a} = 2.105$ and 1.565, respectively. With increasing the gradient parameter γ the mode-I SIF is decreasing. A similar phenomenon is observed for an edge crack in an elastic FGM strip under a mechanical loading (Dolbow and Gosz 2002) and for a cracked piezoelectric FGM strip (Sladek et al. 2007a). For a crack in a homogeneous magnetoelastic solid under a static loading condition as analyzed in the previous example, the mode-I SIF, EDIF and MIIF are uncoupled. However, this conclusion is not valid generally for a continuously nonhomogeneous solid. For the present example, we have obtained the following normalized intensity factors: $\Lambda_d K_D / K_I^{stat} = 0.049$ and $\Lambda_b K_B / K_I^{stat} = 0.0041$. Thus, the material inhomogeneity affects the interactions of the electro-magnetic fields with the mechanical one as compared with the case of homogeneous materials. From the mathematical point of view, one has to solve the boundary value problems described by partial differential equations (PDEs) with variable coefficients for FGMs instead of the PDEs with constant coefficients for homogeneous materials.

Next, the strip is subjected to an impact mechanical load with Heaviside time

variation and the amplitude $\sigma_0 = 1Pa$. The impermeable crack-face boundary conditions for the electrical and magnetic fields are considered. The time variation of the normalized mode-I stress intensity factor is given in Fig. 8, where $K_I^{stat} = 2.64Pa \cdot m^{1/2}$.

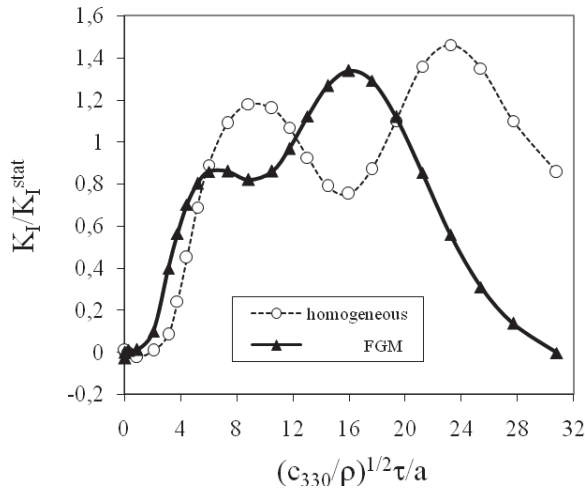


Figure 8: Normalized mode-I stress intensity factor for an edge crack in a strip under a pure mechanical load $\sigma_0 H(\tau - 0)$

The elastic wave velocities are increasing in the x_1 -direction, provided that mechanical parameters of FGMs are increasing in the x_1 -direction and the mass density is uniform. Therefore, the peak values of the mode-I SIF are reached at a shorter time instant in functionally graded strip than in a homogeneous one. The maximum value of the mode-I SIF is reduced for the cracked FGM strip compared to that for a cracked homogeneous strip. Also in this case the EDIF and MIIF have finite values despite a pure mechanical load. The time variations of the EDIF and MIIF are given in Figs. 9 and 10. Again the peak values of the EDIF and MIIF are shifted to shorter time instants in the FGM strip than in a homogeneous one. All three peaks for the SIF, EDIF and MIIF are reached almost at the same time instants.

Finally, it should be noted that in this paper we have analyzed the transient response of a stationary crack in a finite domain under an impact mechanical load with Heaviside time variation. In this case, the dynamic solution does not tend to the static solution when the time t approaches infinity, due to repeated wave reflections at the finite boundaries. In contrast, for the same crack problem but in an infinite domain,

the dynamic solution will tend to the static one in the large-time limit $t = \infty$ as in the purely elastodynamic case.

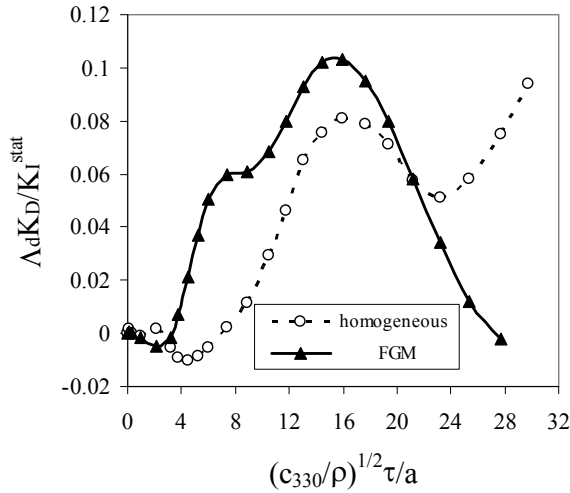


Figure 9: Normalized electrical displacement intensity factors (EDIF) for an edge crack in a strip under a pure mechanical load $\sigma_0 H(\tau - 0)$

6 Conclusions

Stress intensity factors and other intensity factors can be evaluated from asymptotic expansions of the field quantities in the crack-tip vicinity. The validity of the asymptotic expansions is limited to a small region around the crack-tip. If we want to obtain accurate intensity factors we need to get accurate quantities in the crack-tip vicinity. Due to the high gradient of the field quantities in the crack-tip vicinity it is difficult to get accurate quantities there. However, it is possible to develop more sophisticated methods like in this paper, where intensity factors are evaluated on the base of quantities at points far away from the crack-tip.

This paper presents an efficient numerical method for the evaluation of intensity factors for crack problems in magnetoelastoelectric solids. Conservation integral representations for the SIFs, EDIF and MIIF are derived. The present integral method is numerically more expedient than those based on the direct computation of the fracture parameters from the asymptotic expansion of the displacements and potentials. The contour-domain integral approach is well suited for crack analysis

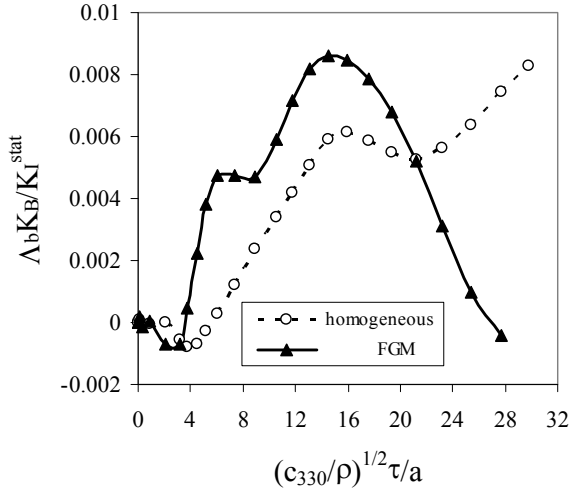


Figure 10: Normalized magnetic induction intensity factors (MIIF) for an edge crack in a strip under a pure mechanical load $\sigma_0 H(\tau - 0)$

by meshless methods. A meshless local Petrov-Galerkin method (MLPG) is applied for 2-D crack problems in continuously nonhomogeneous magnetoelastic solids subjected to a mechanical or magnetic induction loading. Both static and impact loads are considered. The inertial term is considered in the equations of motion. The coupled governing partial differential equations are satisfied in a weak-form on small fictitious subdomains. A unit step function is used as the test function in the local weak-form of the governing partial differential equations on small circular subdomains spread on the analyzed domain. The moving least-squares (MLS) scheme is adopted for the approximation of the physical field quantities. One obtains a system of ordinary differential equations for certain nodal unknowns. That system is solved numerically by the Houbolt finite-difference scheme. The proposed method is a truly meshless method, which requires neither domain elements nor background cells in either the interpolation or the integration. Numerical examples demonstrate the accuracy and the efficiency of the present method.

Acknowledgement: The authors gratefully acknowledge the support by the Slovak Science and Technology Assistance Agency registered under number APVV-0014-10, the Slovak Grant Agency VEGA-2/0039/09, and the German Research Foundation (DFG, Project-No. ZH 15/14-1).

References

- Avellaneda, M., Harshe, G.** (1994): Magnetolectric effect in piezoelectric/magnetostrictive multilayer (2-2) composites. *Journal of Intelligent Material Systems and Structures*, vol. 5, pp. 501-513.
- Atluri, S.N.** (2004): The Meshless Method, (MLPG) For Domain & BIE Discretizations. Tech Science Press, Forsyth.
- Atluri, S.N., Han, Z.D., Shen, S.** (2003): Meshless local Petrov-Galerkin (MLPG) approaches for solving the weakly-singular traction & displacement boundary integral equations. *CMES: Computer Modeling in Engineering & Sciences*, vol. 4, pp. 507-516.
- Banks-Sills, L., Motola, Y., Shemesh, L.** (2008): The M integral for calculating intensity factors of an impermeable crack in a piezoelectric material. *Engn. Fracture Mechanics*, vol. 75, pp. 901-925.
- Bechet, E., Scherzer, M., Kuna, M.** (2009): Application of the X-FEM to fracture of piezoelectric materials. *Int. J. Numerical Meth. Engn.*, vol. 77, pp. 1535-1565.
- Belytschko, T., Krogauz, Y., Organ, D., Fleming, M., Krysl, P.** (1996): Meshless methods; an overview and recent developments. *Comp. Meth. Appl. Mech. Engn.*, vol. 139, pp. 3-47.
- Cherepanov, G.P.** (1979): Mechanics of brittle fracture (Peabody AL, De Wit R, Cooley WC, Trans.). Mac Graw Hill, pp.317-336.
- Dolbow, J.E., Gosz, M.** (2002): On computation of mixed-mode stress intensity factors in functionally graded materials. *Int. J. Solids Structures*, vol. 39, pp. 7065-7078.
- Du, J.K., Shen, Y.P., Ye, D.Y., Yue, F.R.** (2004): Scattering of anti-plane shear waves by a partially debonded magneto-electro-elastic circular inhomogeneity. *International Journal of Engineering Science*, vol. 42, pp. 887-913.
- Eischen, J.W.** (1987): Fracture of nonhomogeneous materials. *Int. J. Fracture*, vol. 34, pp. 3-22.
- Enderlein, M., Ricoeur, A., Kuna, M.** (2005): Finite element techniques for dynamic crack analysis in piezoelectrics. *Int. J. Fracture*, vol. 134, pp. 191-208.
- Feng, W.J., Su, R.K.L.** (2006): Dynamic internal crack problem of a functionally graded magneto-electro-elastic strip. *Int. J. Solids Structures*, vol. 43, pp. 5196-5216.
- Feng, W.J., Su, R.K.L.** (2007): Dynamic fracture behaviors of cracks in a functionally graded magneto-electro-elastic plate. *European Journal of Mechanics A/Solids*, vol. 26, pp. 363-379.

Gao, C.F., Kessler, H., Balke, H. (2003): Crack problems in magnetoelastoelectric solids. Part I: exact solution of a crack. *International Journal of Engineering Science*, vol. 41, pp. 969-981.

Garcia-Sanchez, F., Rojas-Diaz, R., Saez, A., Zhang, Ch. (2007): Fracture of magnetoelastoelectric composite materials using boundary element method (BEM). *Theoretical and Applied Fracture Mechanics*, vol. 47, pp. 192-204.

Garcia-Sanchez, F., Saez, A., Dominguez, J. (2005): Anisotropic and piezoelectric materials fracture analysis by BEM. *Computers & Structures*, vol. 83, pp. 804-820.

Guo, L.F., Li, X., Ding, S.H. (2009): Crack in a bonded functionally graded magneto-electro-elastic strip. *Computational Materials Science*, vol. 46, pp. 452-458.

Han, F., Pan, E., Roy, A.K., Yue, Z.Q. (2006): Responses of piezoelectric, transversely isotropic, functionally graded and multilayered half spaces to uniform circular surface loading. *CMES: Computer Modeling in Engineering & Sciences*, vol. 14, pp. 15-30.

Houbolt, J.C. (1950): A recurrence matrix solution for the dynamic response of elastic aircraft. *Journal of Aeronautical Sciences*, vol. 17, pp. 371-376.

Hu, K.Q., Li, G.Q., Zhong, Z. (2006): Fracture of a rectangular piezoelectromagnetic body. *Mech. Res. Comm.*, vol. 33, pp. 482-492.

Jin, Z.H., Noda, N. (1994): Crack-tip singular fields in nonhomogeneous materials. *ASME Journal of Applied Mechanics*, vol. 61, pp. 738-740.

Kim, J.H., Paulino, G.H. (2003): The interaction integral for fracture of orthotropic functionally graded materials: Evaluation of stress intensity factors. *Int. J. Solids and Structures*, vol. 40, pp. 3967-4001.

Kim, J.H., Paulino, G.H. (2004): T-stress in orthotropic functionally graded materials: Lekhnitskii and Stroh formalisms. *Int. J. Fracture*, vol. 126, pp. 345-384.

Landau, L.D., Lifshitz, E.M. (1984): In: Lifshitz EM, Pitaevskii LP (Eds.), *Electrodynamics of Continuous Media (Second Edition)*. Pergamon Press, New York.

Li, J.Y. (2000): Magnetoelastoelectric multi-inclusion and inhomogeneity problems and their applications in composite materials. *Int. Journal of Engineering Science*, vol. 38, pp. 1993-2011.

Li, S., Liu, W.K. (2004): *Meshfree Particle Methods*. Springer-Verlag (Berlin).

Li, Y.D., Lee, K.Y. (2008): Anti-plane crack intersecting the interface in a bonded smart structure with graded magnetoelastoelectric properties. *Theoretical and Applied Fracture Mechanics*, vol. 50, pp. 235-242.

Liu, G.R., Dai, K.Y., Lim, K.M., Gu, Y.T. (2002): A point interpolation mesh free method for static and frequency analysis of two-dimensional piezoelectric structures. *Computational Mechanics*, vol. 29, pp. 510-519.

Ma, L., Li, J., Abdelmoula, R., Wu, L.Z. (2007): Mode III crack problem in a functionally graded magneto-electro-elastic strip. *Int. Journal of Solids and Structures*, vol. 44, pp. 5518-5537.

Ma, L., Wu, L.Z., Feng, L.P. (2009): Surface crack problem for functionally graded magnetoelastic coating-homogeneous elastic substrate system under anti-plane mechanical and in-plane electric and magnetic loading. *Engineering Fracture Mechanics*, vol. 76, pp. 269-285.

Motola, Y., Banks-Sills, L. (2009): M integral for calculating intensity factors of cracked piezoelectric materials using the exact boundary conditions. *ASME Journal of Applied Mechanics*, vol. 76, 011004.

Nan, C.W. (1994): Magnetolectric effect in composites of piezoelectric and piezomagnetic phases. *Phys. Rev. B*, vol. 50, pp. 6082-6088.

Oh, R.R., Aluru, N.R. (2001): Meshless analysis of piezoelectric devices. *Computational Mechanics*, vol. 27, pp. 23-36.

Pak, Y.E. (1990): Crack extension force in a piezoelectric material. *ASME Journal of Applied Mechanics*, vol. 57, pp. 647-653.

Pak, Y.E., Herrmann, G. (1986): Conservation laws and the material momentum tensor for the elastic dielectric. *Int. J. Engn. Sci.*, vol. 24, pp. 1365-1374.

Parton, V.Z., Kudryavtsev, B.A. (1988): Electromagnetoelasticity, Piezoelectrics and Electrically Conductive Solids. Gordon and Breach Science Publishers, New York.

Paulino, G.H., Jin, Z.H., Dodds, R.H. (2003): Failure of functionally graded materials. In: Karihaloo B, Knauss WG (Eds.), *Comprehensive Structural Integrity*, Volume 2, Elsevier Science, pp. 607-644.

Rao, B.N., Kuna, M. (2008a): Interaction integrals for fracture analysis of functionally graded piezoelectric materials. *Int. Journal of Solids and Structures*, vol. 45, pp. 5237-5257.

Rao, B.N., Kuna, M. (2008b): Interaction integrals for fracture analysis of functionally graded magnetoelastic materials. *Int. J. Fracture*, vol. 153, pp. 15-37.

Sladek, J., Sladek, V., Zhang, Ch., Garcia-Sanchez, F., Wünsche, M. (2006): Meshless local Petrov-Galerkin method for plane piezoelectricity. *CMC: Computers, Materials & Continua*, vol. 4, pp. 109-118.

Sladek, J., Sladek, V., Zhang, Ch., Sulek, P. (2007a): Application of the MLPG

to thermo-piezoelectricity. *CMES: Computer Modeling in Engineering & Sciences*, vol. 22, pp. 217-233.

Sladek, J., Sladek, V., Zhang, Ch., Solek, P., Pan, E. (2007b): Evaluation of fracture parameters in continuously nonhomogeneous piezoelectric solids. *Int. J. Fracture*, vol. 145, pp. 313–326.

Sladek, J.; Sladek, V.; Zhang, Ch.; Wünsche, M. (2010): Crack Analysis in Piezoelectric Solids with Energetically Consistent Boundary Conditions by the MLPG. *CMES: Computer Modeling in Engineering & Sciences*, Vol. 68, No. 2, pp. 185-220.

Sladek, J.; Sladek, V.; Solek, P. (2009): Elastic analysis in 3D anisotropic functionally graded solids by the MLPG. *CMES: Computer Modeling in Engineering & Sciences*, ol. 43, No. 3, pp. 223-252.

Sladek, J., Sladek, V., Solek, P., Pan, E. (2008): Fracture analysis of cracks in magneto-electro-elastic solids by the MLPG. *Computational Mechanics*, vol. 42, pp. 697-714.

Sladek, J.; Sladek, V.; Stanak, P.; Pan, E. (2010): The MLPG for Bending of Electroelastic Plates. *CMES: Computer Modeling in Engineering & Sciences*, Vol. 64, No. 3, pp. 267-298.

Song, Z.F., Sih, G.C. (2003): Crack initiation behavior in magneto-electroelastic composite under in-plane deformation. *Theoretical Applied Fracture Mechanics*, vol. 39, pp. 189-207.

Su, R.K.L., Feng, W.J. (2007): Transient response of interface cracks between dissimilar magneto-electro-elastic strips under out-of-plane mechanical and in-plane magneto-electrical impact loads. *Computers & Structures*, vol. 78, pp. 119-128.

Suresh, S., Mortensen, A. (1998): *Fundamentals of Functionally Graded Materials*, Institute of Materials, London.

Tian, W.Y., Gabbert, U. (2005): Macro-crack-micro-crack interaction problem in magneto-electroelastic solids. *Mech. Mater.*, vol. 37, pp. 565-592.

Tian, W.Y., Rajapakse, R.K.N.D. (2005): Fracture analysis of magneto-electroelastic solids by using path independent integrals. *International Journal of Fracture*, vol. 131, pp. 311-335.

Ueda, S. (2003): Crack in functionally graded piezoelectric strip bonded to elastic surface layers under electromechanical loading. *Theoretical and Applied Fracture Mechanics*, vol. 40, pp. 225-236.

Wang, B.L., Han, J.C., Mai, Y.W. (2006): Mode III fracture of a magneto-electroelastic layer: exact solution and discussion of the crack face electromagnetic boundary conditions. *International Journal of Fracture*, vol. 139, pp. 27-38.

Wang, B.L., Mai, Y.W. (2003): Crack tip field in piezoelectric/piezomagnetic media. *European Journal of Mechanics A/Solids*, vol. 22, pp. 591-602.

Wang, B.L., Mai, Y.W. (2004): Fracture of piezoelectromagnetic materials. *Mech. Res. Comm.*, vol. 31, pp. 65-73.

Wang, B.L., Mai, Y.W. (2007): Applicability of the crack-face electromagnetic boundary conditions for fracture of magneto-electroelastic materials. *Int. J. Solids Structures*, vol. 44, pp. 387-398.

Zhou, Z.G., Wang, B.B., Sun, Y.G. (2004): Two collinear interface cracks in magneto-electro-elastic composites. *Int. Journal of Engineering Sciences*, vol. 42, pp. 1155-1167.

Zhu, X., Wang, Z., Meng, A. (1995): A functionally gradient piezoelectric actuator prepared by metallurgical process in PMN-PZ-PT system. *J. Mater. Sci. Lett.*, vol. 14, pp. 516-518.